Enzymatic Synthesis of Amylose Brushes Revisited

Mazzocchetti, Laura; Tsoufis, Theodorus; Rudolf, Petra; Loos, Katja

Published in:
Macromolecular Bioscience

DOI:
10.1002/mabi.201300273

Publication date:
2014

Enzymatic Synthesis of Amylose Brushes Revisited: Details from X-Ray Photoelectron Spectroscopy and Spectroscopic Ellipsometry[a]

Laura Mazzocchetti, Theodoros Tsoufis, Petra Rudolf,* Katja Loos*

The successful synthesis of amylose brushes via enzymatic "grafting from" polymerization and the detailed characterization of all synthetic steps by X-ray photoelectron spectroscopy (XPS) and spectroscopic ellipsometry measurements are reported. Au and Si surfaces are amino-functionalized with self-assembled monolayers (SAMs) of cystamine and 3-aminopropyldimethyethoxysilane (APDMES), respectively. Maltoheptaose is covalently attached to the amino-functionalized Au and Si surfaces via reductive amination. Amylose brushes are grown from maltoheptaose modified Au and Si surfaces with enzymatic polymerization using potato phosphorylase and Rabbit Muscle phosphorylase, as evidenced by spectroscopic ellipsometry and XPS measurements.

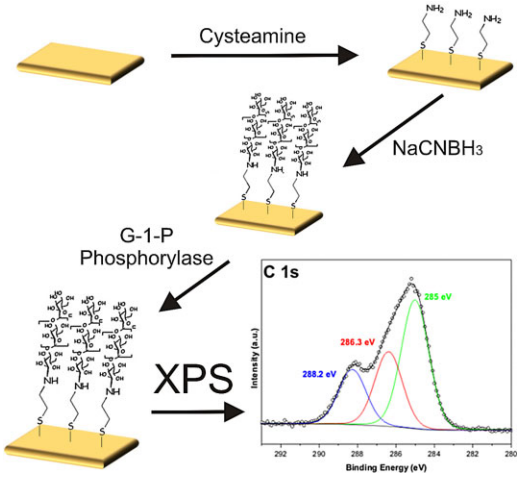

1. Introduction

Polysaccharides are naturally occurring polymers which are mainly renowned for their industrial importance in many fields, such as food processing, packaging and textiles.[1] However, they also attracted some interest in the field of advanced materials due to their biocompatibility, biodegradability and environmental friendliness.[2–4] Moreover, they are rich in free hydroxyl moieties, allowing for water solubility as well as for possible further functionalization of the polymer backbone.

Dr. L. Mazzocchetti, Dr. T. Tsoufis, Prof. P. Rudolf, Prof. K. Loos
Zernike Institute for Advanced Materials, University of Groningen, Nijenborgh 4, NL-9747 AG Groningen, The Netherlands
E-mail: p.rudolf@rug.nl; k.u.loos@rug.nl

[a]**Supporting Information** is available from the Wiley Online Library or from the author.

A particularly interesting aspect of the use of polysaccharides is the prevention of biofouling. The term "biofouling" refers to undesired accumulation of biological molecules, and in some cases of living organisms, on a surface.[5] This phenomenon may occur in different situations, such as in underwater pipes or on ship's hulls,[6,7] in filtration or processing devices in the food industry[8,9] or in biomedical implants.[9] In all these cases the biofilm formation leads to performance losses and, in the case of body implants, to an inflammatory response. The easiest way to avoid or delay biofilm formation is to create a surface that hinders the adsorption of biomolecules, proteins in particular.[7] Owing to the hydrophilic character of polysaccharides they can be used as hydrophilic coating. Indeed it was demonstrated that a hydrophilic surface can prevent, or at least reduce, protein adsorption.[10–12] While poly(ethylene glycol) modified (PEGylated) surfaces showed good results in coating,[13–15] the possibility of using naturally occurring polymers such as polysaccharides may be a superior and more environmental friendly alternative.

DOI: 10.1002/mabi.201300273

Polysaccharide coatings were already successfully produced by selectively adsorbing polysaccharide containing block copolymers on surfaces[16] and the protein repellency of the produced polysaccharide brushes was studied.[17] By covalent attachment of the polysaccharides to the surface the coating properties can be further improved. Two methods are available for the successful synthesis of such so-called polysaccharide brushes: "grafting to" and "grafting from".[18–20] In the "grafting to" approach brushes are prepared by grafting polymers onto surfaces by chemical bonding of functional surface groups to reactive chain ends of the polymers. This method has the disadvantage that it is very difficult to achieve high grafting densities and/or thicker films due to steric crowding of reactive surface sites by already adsorbed polymers. Well-defined polymer brushes can be therefore more elegantly synthesized via a "grafting from" approach, where polymers are grown from surface-bound initiators. The so-called 'grafting from' approach is a superior alternative because the functionality, density and thickness of the polymer brushes can be controlled with almost molecular precision (when utilizing controlled/living polymerization techniques).

Here we present the synthesis and the exact characterization of amylose brushes. Amylose, one of the components of starch, is a linear biomacromolecule in which the glucose units are joined via α-(1→4) glucosyl linkages. Conventional synthetic approaches are, in many cases, inadequate to provide substantial quantities of polysaccharides such as amylose because of difficulties arising from incomplete regio- and stereo-control of the glycosylating process. Enzymatic synthesis methods are very attractive for their mild reaction conditions, for the high enantio-, regio- and chemoselectivity as well as for the nontoxicity of natural catalysts.[21–24] In enzymatic methods for glycoside and saccharide synthesis no selective protection/deprotection steps are necessary and the control of configuration at newly formed anomeric centers is absolute.[25–29]

Interestingly, the first surface-initiated enzymatic polymerization ever reported was the synthesis of amylose brushes on planar and spherical surfaces[30,31] and this approach was extended recently by the synthesis of amylopectin brushes via an enzymatic "grafting from" procedure.[32] However, to date a proper surface chemistry characterization of these systems is still missing.

Here we report the detailed stepwise synthesis and characterization of amylose brushes via an enzymatic "grafting from" polymerization from silica and gold surfaces using α-glucan phosphorylase (E.C. 2.4.1.1) as catalyst. In vivo phosphorylase is involved in the phosphorolytical cleavage of the non-reducing end-unit from α-glucan chains, producing glucose-1-phosphate (G-1-P). However, under the appropriate conditions the catalytic action of phosphorylase can be reverted and linear synthetic amylose can be synthesized with the release of inorganic phosphate.[33–35]

The strict primer dependence of the glycogen phosphorylases makes them ideal candidates for the synthesis of hybrid structures of amylose with non-natural materials.[36–42] For this, a primer functionality (malto-oligosaccharide) can be coupled to a synthetic structure and subsequently elongated by enzymatic polymerization to result in amylose blocks.

The synthetic procedure for the reported amylose brushes is outlined in Figure 1. Silica and gold surfaces were amino-functionalized by reactions with 3-aminopropyldimethylethoxysilane (APDMES) (Figure 1, upper row) and cystamine (Figure 1, lower row), respectively. The primer recognition unit for the enzymatic polymerization (maltoheptaose) is attached to the amino-functionalized surface via reductive amination.[43,44] The primer recognition unit is subsequently elongated in an enzymatic "grafting from" polymerization using phosphorylase as catalyst and G-1-P as monomer.

All synthetic steps were characterized in great depth by X-ray photoelectron spectroscopy (XPS) and spectroscopic ellipsometry measurements confirming the successful step-by-step growth of the amylose brushes via enzymatic polymerization.

2. Experimental Section

2.1. Materials

Double side polished silicon wafers were purchased from TOPSIL (Frederikssund, Denmark). Toluene (Labscan) was freshly distilled from sodium and dimethylsulfoxide (DMSO; Labscan) was distilled from CaH_2. Sodium cyanoborohydride, APDMES, cystamine, Rabbit Muscle phosphorylase *b* (RMP *b*), dithio-D,L-threitol (DTT), TWEEN® 80 (TWEEN) and adenosine 5'-monophosphate (AMP), were all purchased from Aldrich and used as received. Maltoheptaose (MH),[35,37,45] Maltoheptaonolactone[35,37,41] and Potato phosphorylase (PP)[35,37,41] were obtained according to procedures reported in the literature.

2.2. Si Wafer Amination with APDMES

Si wafers were cut in pieces of roughly 1 cm × 2 cm and ultrasonically rinsed with ethanol, ethanol/dichloromethane (50/50) and dichloromethane and finally immerged in a piranha solution (3:1 H_2SO_4:H_2O_2) at 75 °C. After 1 h, the substrates were dropped in Milli Q water, extensively rinsed with Milli Q water and subsequently sonicated with Milli Q water, methanol and toluene. The freshly cleaned Si wafers were soaked in a 0.010 M APDMES solution in freshly distilled toluene at room temperature in a shaking incubator. After 5 h the substrates were rinsed with toluene and placed in a Soxhlet apparatus for 24 h to remove the unreacted APDMES. Finally the substrates were baked at 120 °C for 1 h.

2.3. Gold Substrate Functionalization with Cystamine

150 nm thick polycrystalline gold films on mica (grade V-1, Ted Pella) were prepared in a home-built deposition system

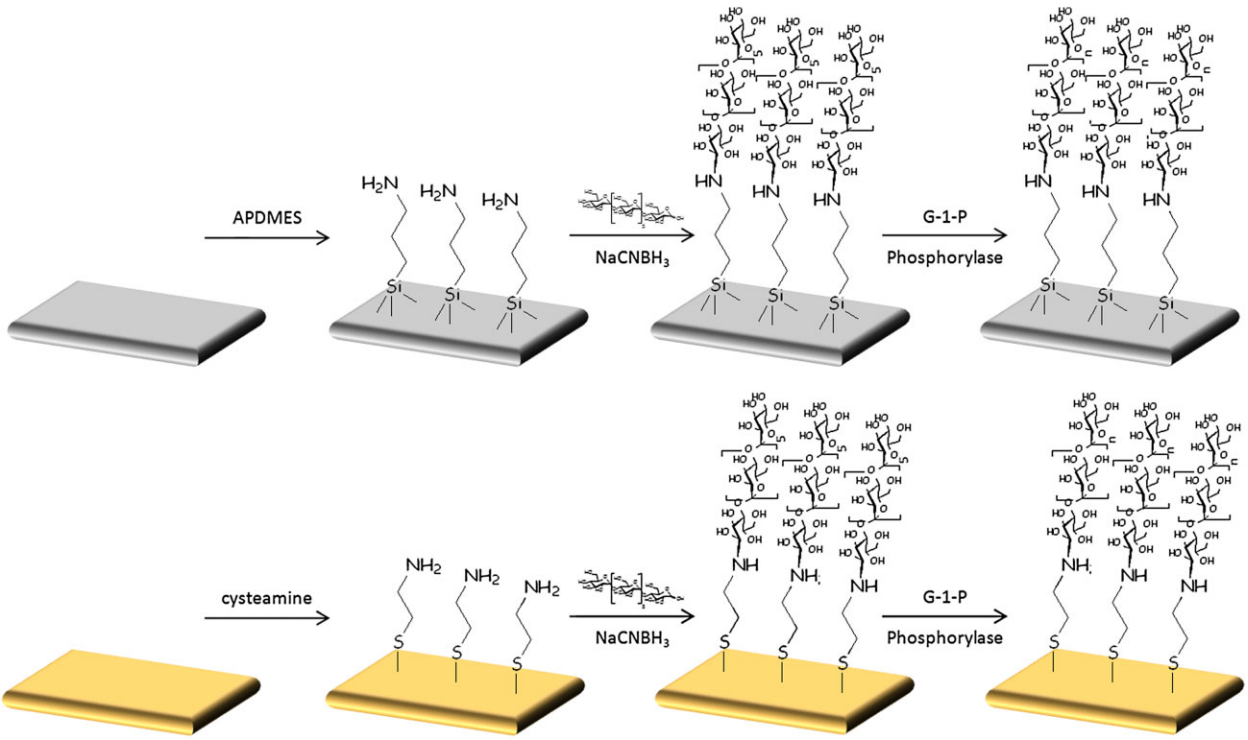

Figure 1. Synthesis of amylose brushes via enzymatic "grafting from" polymerization from silica (upper row) and gold surfaces (lower row).

by sublimation of 99.99% gold (Schöne Edelmetaal B.V.). To obtain atomically flat Au(111) substrates, sublimation was carried out at a base pressure of 10^{-7} Torr onto freshly cleaved mica sheets kept at 650 K, which had been pre-heated at the same temperature for 16 h in order to degas environmental impurities. The substrates were cooled down to room temperature over a period of 8 h. Freshly prepared gold surfaces were functionalized by submerging them in a degassed 0.010 M ethanol or aqueous solutions of cystamine. The surfaces were allowed to react for 18 h in the dark at room temperature under a N_2 atmosphere. Subsequently the surfaces were removed from the solution, washed twice with ethanol and water and dried.

2.4. Reductive Amination

The amino functionalized surfaces were submerged in a DMSO solution containing 1 vol% acetic acid, 10 mg mL^{-1} MH, 2.5 mg mL^{-1} $NaCNBH_3$ and 4 Å molecular sieves. The reductive amination was carried out at a temperature of 60 °C for 3 d in a shaking incubator. Substrates were rinsed extensively with Milli Q water after reaction and subsequently sonicated with Milli Q water and ethanol.

2.5. Enzymatic Polymerization with PP

MH functionalized samples were submerged in citrate buffer (pH 6.2, 0.050 M) solution containing G-1-P (250×10^{-9} M) and phosphorylase (5 U mL^{-1}). Samples were allowed to react for 3 d at 38 °C in a shaking incubator. Afterwards the substrates where cleaned with different cleaning procedures. 1) Flushing with Milli Q water and subsequent sonication in Milli Q water; 2) Flushing with Milli Q water and subsequent sonication in water, DMSO, acetone, methanol and heptane; 3) Flushing with Milli Q water and subsequent sonication in Milli Q water; 2) Flushing with Milli Q water and subsequent sonication in water, DMSO, acetone, methanol and heptane; 3) Flushing with Milli Q water and subsequent sonication with tris-buffered saline (TBS) with 2% TWEEN, followed by rinsing with plain Milli Q water; the process was repeated twice, followed by 6 more cycles with no TWEEN addition. Finally samples were sonicated in DMSO and in Milli Q water. At the end of each cleaning procedure all the samples were dried at 105 °C for 1 h.

2.6. Enzymatic Polymerization with RMP b

MH functionalized samples were submerged in 2-amino-2-(hydroxymethyl)-propan-1,3-diol (TRIS) buffer (pH 6.7, 0.1 M) solution containing G-1-P (0.250 M), AMP (0.04 M), DTT (0.04 M) and RMP *b* (2.5 U · mL^{-1}). Samples were allowed to react for 4 d at 38 °C in a shaking incubator. Afterwards the substrates where cleaned by flushing with Milli Q water and sonication in Milli Q water, DMSO, acetone, methanol and heptane.

2.7. Methods of Characterization

2.7.1. Spectroscopic Ellipsometry

Spectroscopic ellipsometry was performed on a VASE VB-400 ellipsometer in the range of 400 to 1000 nm. The angle of incidence

was varied between 74° and 76° in 1° steps. The software package WVASE32 was used to make a model consisting of different layers with characteristic values for the refractive indices. A Cauchy dispersion layer was used to determine the thickness of the APDMES, maltoheptaose and polysaccharide layer. The refractive index of maltoheptaose and of the α-glucan brush was taken to be 1.336, that of APDMES 1.465.[46]

2.7.2. XPS

For the XPS measurements, evaporated gold films supported on mica were used as substrates. Samples were introduced via a load lock system into a SSX-100 (Surface Science Instruments) photoelectron spectrometer with a monochromatic Al-K_α X-ray source ($h\nu = 1486.6$ eV). The base pressure in the spectrometer was 1×10^{-10} Torr during all measurements. The energy resolution was set to 1.16 eV to minimize the measuring time. The photoelectron take-off angle was 37°. All binding energies were referenced to the Au $4f_{7/2}$ core level.[47] Spectral analysis included a Shirley background subtraction in the case of carbon 1*s* core level spectrum and a linear background in the case of nitrogen 1*s* and sulfur $2p_{3/2}$ spectra due to high signal to noise ratio.[48] Peak deconvolution included mixed Gaussian – Lorentzian functions in a least squares curve-fitting program (WinSpec) developed at the University of Namur, Belgium. The procedure consisted in fitting a minimum number of peaks that can reproduce the raw data and are consistent with the experimental resolution and the molecular structure of the thin films. All measurements were performed on freshly prepared samples in order to guarantee the reproducibility of the results. Three different points on each sample were analyzed to check for homogeneity. The photoemission peak intensities of each element, used to estimate the amount of each species on the surface, were normalized by the sensitivity factors of each element tabulated for the spectrometer used. The error on the photoemission peak intensities was estimated depending on the signal-to-noise ratio in the spectrum for each element. The carbon signal was better defined; thus the error was found to be 2%. The nitrogen and sulfur signals were weaker, producing noisier spectra, and therefore a more substantial error of 5% and 6% was estimated in the corresponding peak intensities. The stability of the self-assembled monolayers (SAMs) of cystamine on gold (and of the films grown on them) to damage induced by the X-ray beam and by secondary electrons produced by photoemission in the underlying substrate was explored by monitoring the line shape and relative intensity of the C 1*s*, N 1*s*, and S $2p_{3/2}$ core-levels as a function of irradiation time. No evidence of structural degradation was observed even when irradiation was continued twice as long as the acquisition time used in the measurements.

3. Results and Discussion

Amylose brushes were successfully synthesized via an enzymatic "grafting from" polymerization (see Figure 1).

3.1. Amino-Functionalized Surfaces

The reaction starts with the functional modification of surfaces via the introduction of a convenient functional group. In the present case, the functional group chosen for the primer attachment is the amine moiety, so both gold and double-sided polished Si wafer substrates were functionalized with SAMs of molecules bearing amine functionality on one side and a surface linker on the other (see Figure 1). Cystamine was used for self-assembly on gold while the functionalization of Si wafers was carried out with APDMES, a monoalkoxy-silane derivative. In both cases the aliphatic chain spacer between the surface linker and the amine group had three methylene units. From ellipsometric measurements the thickness of the cystamine SAM on Au was found to be 0.60 ± 0.07 nm while that of the APDMES SAM on Si amounted to 0.65 ± 0.08 nm, in accordance with literature data for uniform SAMs.[49]

XPS studies of the surfaces confirm the presence of amine groups anchored to an aliphatic chain (see Supporting Information file for the XPS spectra of the APDMES SAM on Si, Figures S1,S2). The effect of the solvent on the structure of the resulting SAMs of cystamine on gold was studied by XPS. When the self-assembly took place from an ethanol solution, the nitrogen 1*s* core level region of the XPS spectra revealed the presence of two different chemical species (Figure 2, left), one at 399.8 eV binding energy which is attributed to the presence of free amines and accounted for 56% of the total nitrogen intensity, and another component at 401.6 eV, attributed[50] to protonated amines (NH_3^+) and corresponding to approximately the 44% of the overall nitrogen intensity. The sulfur 2*p* region of the XPS spectrum (Figure 2, right) showed two major components corresponding to different chemical environments neighboring sulfur atoms. The sulfur $2p_{3/2}$ component at 162.3 eV is due to the sulfur atoms bound to gold.[51] The second sulfur component at 168.2 eV, is attributed to oxidized sulfur species[52] that remained on the surface after washing. As the oxidized sulfur species are negatively charged, these species are expected to remain in the monolayer even after extensive washing due to interactions with, for example, charged amino groups as reported in similar self-assembled films.[53]

XPS can provide not only qualitative but also quantitative information.[54] In fact, the peak intensities normalized with the atomic sensitivity factors are proportional to the amount of the corresponding atoms within the sampling depth. The recorded ratio between the peak intensities of nitrogen and sulfur for the SAM of cystamine on gold was 0.98, that is, within the experimental error equal to the expected value (1) for cystamine.

When the self-assembly of cystamine on gold took place from aqueous solution, significant changes were noted in the XPS spectrum of the formed SAM. In detail, the high resolution nitrogen 1*s* spectrum (Figure 3, left) revealed again two major components for free and protonated amines (recorded at 399.4 and 400.9 eV, respectively) shifted to lower binding energies when compared to the

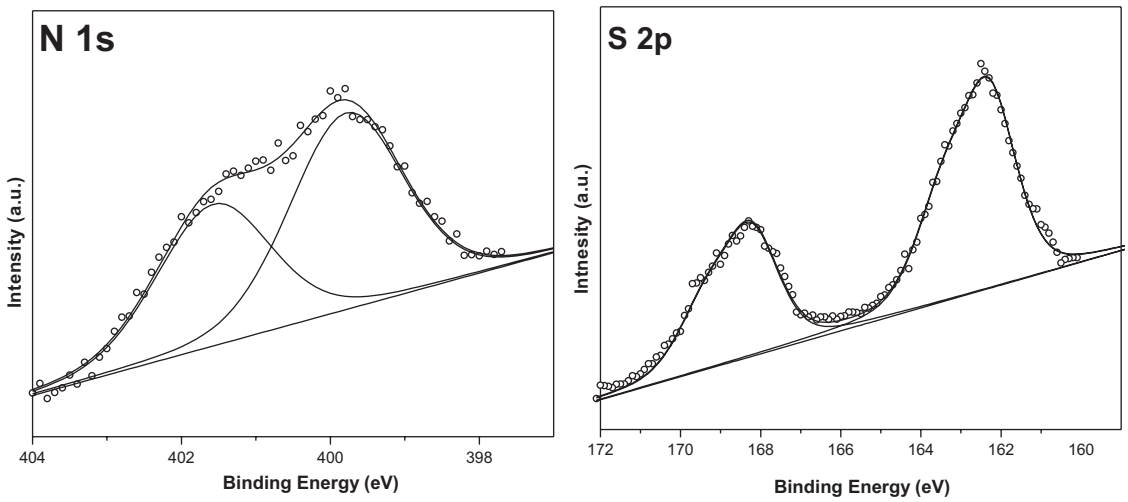

Figure 2. N 1*s* (left) and S 2*p* (right) core level XPS spectra of cystamine monolayers on gold self-assembled from an ethanol solution.

case of self-assembly from an ethanol solution. However, the ratio of peak intensities corresponding to free and protonated amines was found significantly higher (1.9) in the case of the SAM cystamine assembled in water than for the self-assembled monolayer in ethanol (1.2). This finding indicates that self-assembly from water solutions results in SAMs with a significantly higher percentage of free amine terminal groups, in agreement with previous reported results from our group[46] and others.[55] The sulfur 2*p* region (Figure 3, right) in the XPS spectrum of these SAMs showed three different components. The dominant component, recorded at 161.9 eV originates from sulfur atoms bonded to gold, while the two additional minor contributions at 165.2 eV and 168.3 eV are both attributed to oxidized sulfur species that remain present at the gold surface. As for the SAM assembled in ethanol solution, also for the SAM assembled in water solution, the ratio between the N 1*s* to S 2*p* peak intensities was 0.99, i.e. within the experimental error equal to the expected value (1) for cystamine.

3.2. Maltoheptaose-Functionalized Surfaces

As previously stated, for phosphorylase to catalyze the enzymatic "grafting from" polymerization of G-1-P a primer recognition unit of at least 3 $\alpha(1\rightarrow4)$ connected glucose units is required. Here, maltoheptaose, a seven-glucose oligomer, was used as primer and attached to the aminated surfaces via reductive amination with $NaCNBH_3$ (see Figure 1).

Spectroscopic ellipsometry measurements shows that a dense maltoheptaose layer forms on gold substrate of about 2.5 ± 0.12 nm, while on Si wafer the layer thickness is about 1.6 ± 0.3 nm. While the MH layer grown on gold/

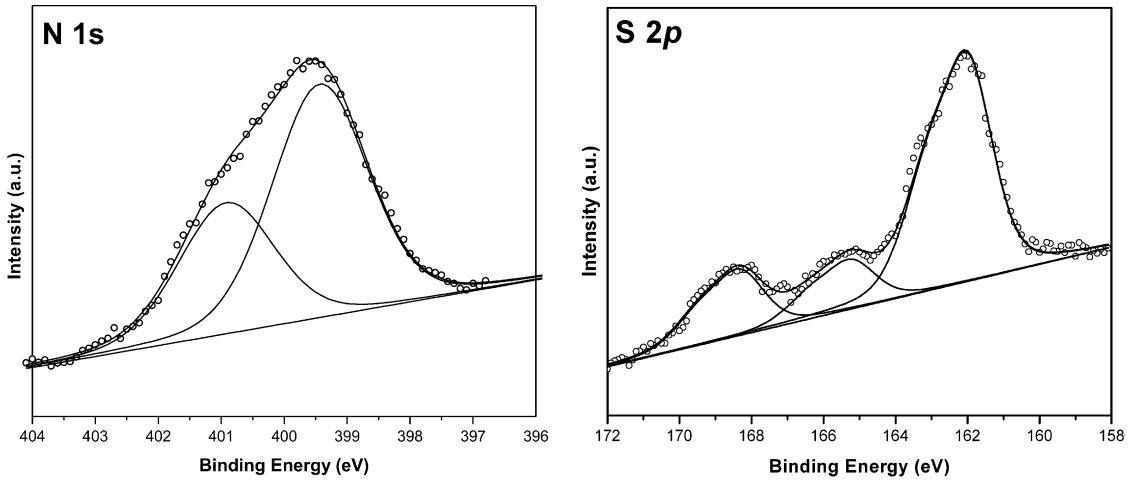

Figure 3. Nitrogen 1*s* (left) and sulfur 2*p* (right) core level XPS spectra of cystamine monolayers on gold self-assembled from water solution.

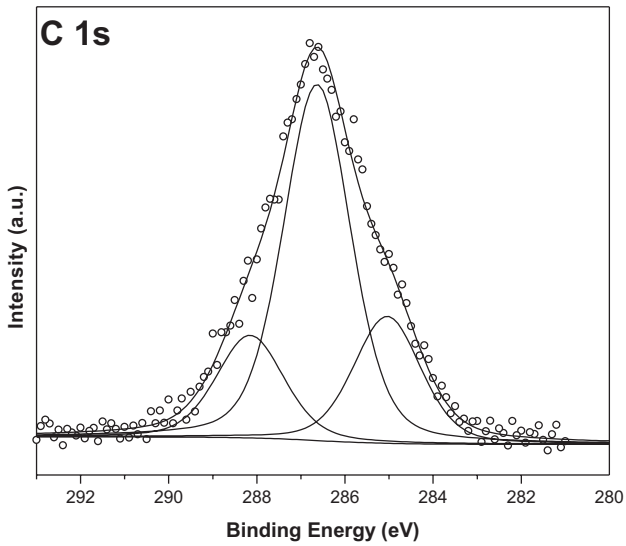

Figure 4. C 1*s* core level region of the photoemission spectrum of maltoheptaose immobilized on a cystamine SAM on gold.

cysteamine substrates compare well with the dimension of an extended MH unit, the thickness measured on Si wafer/APDMES is well below the value found for a similar system in which the Si wafer was functionalized with 3-aminopropyltriethoxysilane (APTES), that was reported to be about 3.5 nm.[22] According to literature reports, the amine density obtained by funtionalization with APDMES and APTES is quite different, being 1.6 NH_2 nm^{-2} and 4.0 NH_2 nm^{-2}, respectively, owing to the possibility of the latter of giving multilayer self-assembly instead of a strict monolayer formation. When the MH density on the surface is calculated according to Equation 1:

$$\sigma = L\rho N_A/M_n \quad (1)$$

from the layer thickness L, the density of maltoheptaose ρ, and its molecular weight M_n, and given the Avogadro constant N_A, the results show 0.9 MH nm^{-2} and 1.9 MH nm^{-2} respectively in the case of Si wafers functionalized with APDMES and APTES, evidencing that in both cases only roughly 50% of the amine groups present on the surface are able to react with the primer.

The XPS carbon 1*s* spectrum of maltoheptaose immobilized on the cystamine SAM on gold is presented in Figure 4 (see Supporting Information file for the XPS spectra of maltoheptaose immobilized on the APDMES SAM on Si, Figures S3,S4). Three different components were necessary to fit the spectrum. The highest binding energy component at 288.1 eV is attributed to the acetal carbon atoms (O–C–O) present at the maltoheptaose structure, while the major component at 286.6 eV originates from the ether (C–O–C) and alcohol (C–O–H) contributions also present in maltoheptaose. Nevertheless, additional contributions to this component may come from C–N bonds formed during the reaction of the amine-terminated SAM with the maltoheptaose. This hypothesis is further supported by the detailed analysis of the nitrogen region, discussed below. The lowest binding energy component at 285 eV is attributed to the C–C moieties of the aliphatic chains of cystamine as well as to adventitious hydrocarbon contamination. The latter is supported by the significantly higher relative intensity of this component with respect to what is expected based on stoichiometry.

The successful attachment of maltoheptaose to the SAM-functionalized gold was further evidenced in the nitrogen 1*s* core level XPS spectrum (Figure 5, left). Apart from the previously noted components of free and protonated amines at 399.7 and 401.6 eV, an additional component not present in the corresponding spectrum of the cystamine SAM on gold, was found at 399 eV. This

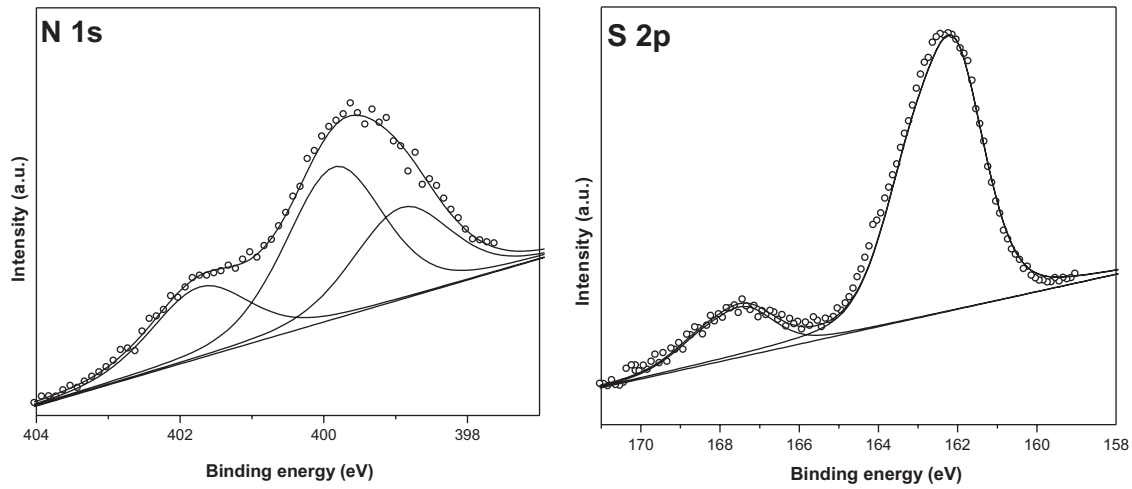

Figure 5. N 1*s* (left) and S 2*p* (right) core level regions of the photoemission spectrum of maltoheptaose immobilized on a cystamine SAM on gold.

additional component, which amounts to 25% of the overall nitrogen intensity, is attributed to the formation of the secondary amine bond formed by the reaction between the maltoheptaose and the SAM of cystamine. The analysis of the XPS results further suggests that the attachment of the maltoheptaose took place preferably onto the free amine groups as expected, since the relative percentage of the protonated amines compared to the total nitrogen intensity, before and after the immobilization of maltoheptaose remained practically the same (ca. 30%). Furthermore, the XPS results (Figure 5, right) pointed out that the relative intensity of the oxidized sulfur species was significantly reduced after the reaction. In fact, the relative intensity due to the oxidized sulfur species now corresponds to only 14% of the total sulfur intensity, compared to the 34% before the reaction took place. No significant difference was observed in the maltoheptaose attachment onto aminated gold or aminated silicon wafers. It is worth noting instead that the only significant parameter affecting the success and extent of the reductive amination was the ratio of free vs. protonated amine groups. When the aminated surfaces are dominated by protonated amine groups (more than 60% of total nitrogen intensity), no significant maltheptaose attachment is observed, while the reaction proceeds smoothly when the free amine groups are the majority on the surface (around 60% of the total nitrogen intensity).

3.3. Amylose-Functionalized Surfaces

Once the primer is attached to the surface, polymerization of G-1-P can be carried out in the presence of α-glucan phosphorylase. This enzyme is naturally found in many living organisms, and it can be isolated form a number of them. One of the most common sources of α-glucan phosphorylase is potatoes. The enzyme extracted from the tuber is in its active form, without any need for regulatory mechanism; thus, no addition of co-factors is required to drive the polymerization. Nevertheless, the extraction procedure from the potato juice carries along many contaminants that, although not interfering with the α-1,4-glycosidic bond formation, contaminate the final products. The polymerization is carried out for 3 d, since no further increase in the brushes degree of polymerization was observed at longer incubation time.[28] Samples were cleaned by simple flushing and sonicating with water. While the spectroscopic ellipsometry detected an average increase in the carbohydrate average layer thickness, the actual thickness strongly depends on the initial substrate used for functionalization. On gold/cysteamine an average brush layer of about 20.0 ± 1.9 nm could be obtained, while on the Si wafer/APDMES surface the layer was considerably thinner, measuring about 6.0 ± 0.8 nm. This result reflects the previously outlined differences observed for MH functionalization on the different supporting systems. While on the gold/cysteamine surface extended MH units can be assumed, the lower density obtained on Si wafer/APDMES can envisage the presence of some coiled units that makes them inaccessible for further polymerization. The degree of polymerization of the amylose brushes can be estimates as previously reported.[32]

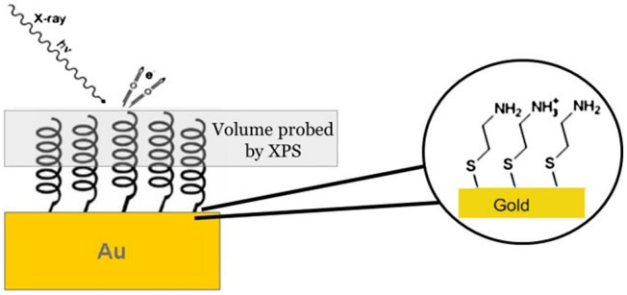

Figure 6. Proposed schematic representation of XPS probed top-section of amylose brushes.

A first proof of the successful brush growth was provided from the XPS spectra after the enzymatic polymerization. In detail, the XPS results did not reveal any contribution either from sulfur $2p_{3/2}$ or from gold $4f_{7/2}$ core level regions. This is not surprising given the fact that XPS is a surface sensitive technique and although the X-rays can penetrate to the bottom section, the electrons cannot go through the thick upper layer (see Figure 6 for a schematic outline).

Surprisingly, a nitrogen peak was recorded, although not expected as the presence of nitrogen is only limited to the "root" of the brushes (Figure 6, insert). These observations suggest the presence of N-containing contaminants entrapped within the brushes, which might probably stem from proteic residues coming along with the potato extracted enzyme.

Hence, different methods were applied to remove the contaminants form the brushes, and besides the simple sonication in water, a sequence of sonicating sessions in a combination of water/organic solvents (dimethylsulfoxide, water, acetone, methanol, heptane), and the use of surfactants to remove the proteic residues were attempted. The most effective way to remove contaminants from the brushes is the subsequent washing with a series of different solvents, which results in a relative intensity ratio of C to N ratio of 16, while with the other processes the C/N ratio is around 10. The method is however not completely efficient (see Figure 7a–c).

Given the fact that no complete removal of absorbed proteic residues was accomplished when Potato phosphorylase (PP) was used as catalyst, commercial Rabbit Muscle phosphorylase *b* (RMP *b*) was used to carry out the enzymatic "grafting from" polymerization. While PP and

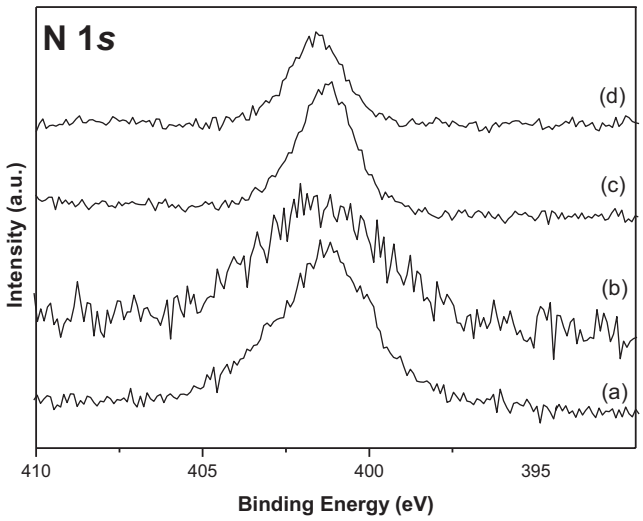

Figure 7. XPS spectra of the N 1*s* core level regions of amylose brushes grown using PP enzyme and treated with a) water, b) TBS and Tween, c) a combination of aquatic and organic solvents, and d) brushes grown using RMP *b* and cleaning with a combination of aquatic and organic solvents.

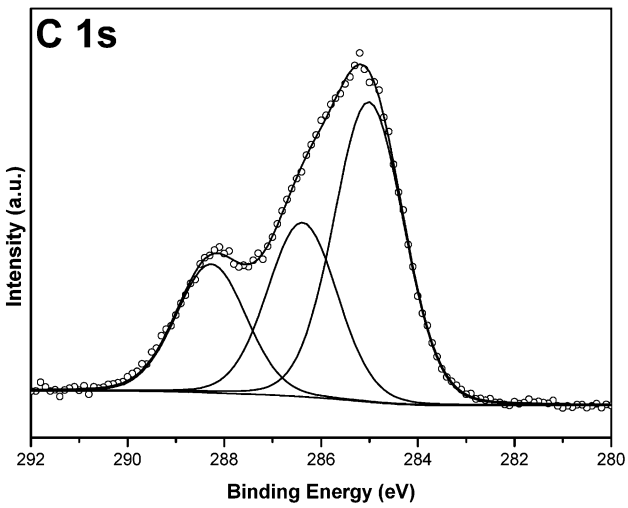

Figure 8. C 1*s* core level XPS spectrum of amylose brushes grown by the enzymatic polymerization of MH functionalized Au surfaces using RMP *b*.

RMPs (EC 2.4.1.1) are similar in many structural and kinetics characteristics, the later exists in two forms, *a* and *b* respectively, that require allosteric and covalent control mechanisms.[56] In particular, RMP *b* requires the presence of AMP for having a catalytic activity.[57] Another important difference between PP and RMP lies in the affinity for different glucan substrates: while the first one shows preference for linear polysaccharides, the latter acts preferentially on branched glucans. We recently successfully used RMP *b* for the synthesis of well-defined linear and branched polyglucans.[58–60]

RMP *b* can also be used for the enzymatic "grafting from" polymerization of amylose brushes. With this the amount of absorbed proteic residues can be further reduced, see Figure 7d. The carbon *1s* core level XPS spectrum of amylose brushes grown by the enzymatic polymerization with RMP *b* on gold clearly proves the successful synthesis of the amylose brush, see Figure 8. The spectrum is constituted by three components. The highest binding energy component, recorded at 288.2 eV is attributed to the O–C–O bonds and corresponds to 22% of the total carbon intensity. The two other components originate from C–OH at 286.3 eV (28% of the overall C intensity) and at 285.0 eV (50% of the overall C intensity), respectively.

The split of the C–OH signal results from differences in hydrogen bonding along the amylose helix. The stability of a V-amylose helical structure essentially relies on intra-molecular hydrogen bonds, (distinguishable into two types of hydrogen bonds that are defined as interturn H bonds (O6–O2 and O6–O3) and intraturn H bonds between adjacent glucose units (O2–O3), respectively.[61–66] It is known that differences in strength of hydrogen bonds contribute differently to the core level binding energies assessed by XPS[67] and we can therefore clearly distinguish the interturn H bonds (285.0 eV) and intraturn H bonds (286.3 eV) in the C 1*s* core level XPS spectrum of the synthesized amylose brushes (see Figure 8). The measured percentages of O–C–O, C–OH interturn H bonds and C–OH intraturn H bonds agree well with theoretically calculated percentages of O–C–O, 15.6% of the total carbon and C–OH interturn H bonds, 53.3% of the total carbon and C–OH intraturn H bonds, 29.2% of the total carbon.

Amylose brushes were also successfully synthesized on Si surfaces, see Supporting Information file for the XPS spectra (Figures S5,S6).

4. Conclusion

Amylose brushes on Au and Si surfaces were successfully synthesized via enzymatic polymerization using PP and RMP. The synthetic procedure involved amino-functionalization of the surfaces via SAMs, covalent attachment of MH to the functionalized surfaces via reductive amination and subsequent enzymatic "grafting from" polymerization. The in-depth characterization of all synthetic steps by XPS and spectroscopic ellipsometry measurements proved the feasibility of the synthetic protocol and evidenced distinct differences such as variances in surface coverage depending on the SAM used. Less proteic contamination in the amylose brushes resulted when utilizing phosphorylase from Rabbit Muscles in contrast to phosphorylase extracted from potatoes.

Acknowledgements: Financial support of this research by the Foundation for Fundamental research on Matter (FOM) programme 'Bio(-related) materials' under project number 08BRM12 is greatly acknowledged.

Received: May 31, 2013; Revised: July 29, 2013; Published online: October 8, 2013; DOI: 10.1002/mabi.201300273

Keywords: amylose brushes; ellipsometry; enzymatic polymerization; self-assembled monolayers; x-ray photonelectron spectroscopy

[1] A. Buléon, P. Colonna, V. Planchot, S. Ball, *Int. J. Biol. Macromol.* **1998**, *23*, 85.
[2] K. Kumar, A. J. J. Woortman, K. Loos, *Biomacromolecules* **2013**, *14*, 1955.
[3] R. Rachmawati, A. J. J. Woortman, K. Loos, *Macromol. Biosci.* **2013**, *13*, 767.
[4] R. Rachmawati, A. J. J. Woortman, K. Loos, *Biomacromolecules* **2013**, *14*, 575.
[5] L. F. Melo, T. R. Bott, *Exp. Thermal Fluid Sci.* **1997**, *14*, 375–381.
[6] D. L. Schmidt, R. F. Brady, K. Lam, D. C. Schmidt, M. K. Chaudhury, *Langmuir* **2004**, *20*, 2830.
[7] M. Krivorot, A. Kushmaro, Y. Oren, J. Gilron, *J. Membrane Sci.* **2011**, *376*, 15.
[8] H. C. Flemming, T. Griebe, G. Schaule, *Water Sci. Technol.* **1996**, *34*, 517.
[9] R. D. Frank, H. Dresbach, H. Thelen, H. G. Sieberth, *J. Biomed. Mater. Res.* **2000**, *52*, 374.
[10] S. Chen, L. Li, C. Zhao, J. Zheng, *Polymer* **2010**, *51*, 5283.
[11] M. Amiji, K. Park, *Biomaterials* **1992**, *13*, 682.
[12] Y. C. Tseng, T. McPherson, C. S. Yuan, K. Park, *Biomaterials* **1995**, *16*, 963.
[13] N. V. Efremova, S. R. Sheth, D. E. Leckband, *Langmuir* **2001**, *17*, 7628.
[14] K. Kawasaki, M. Kambara, H. Matsumura, W. Norde, *Biofouling* **2003**, *19*, 355.
[15] T. McPherson, A. Kidane, I. Szleifer, K. Park, *Langmuir* **1998**, *14*, 176.
[16] W. T. E. Bosker, K. Agoston, M. A. Cohen Stuart, W. Norde, J. W. Timmermans, T. M. Slaghek, *Macromolecules* **2003**, *36*, 1982.
[17] W. T. E. Bosker, K. Patzsch, M. A. C. Stuart, W. Norde, *Soft Matter* **2007**, *3*, 754.
[18] R. Jordan, *Surface-Initiated Polymerization I*, Springer, Berlin/New York **2006**, Vol. 197.
[19] R. Jordan, *Surface-Initiated Polymerization II*, Springer, Berlin/New York **2006**, Vol. 198.
[20] S. J. Peng, B. Bhushan, *RSC Adv.* **2012**, *2*, 8557.
[21] K. Loos, *Biocatalysis in Polymer Chemistry*, Wiley, New York/Chichester, UK **2010**.
[22] A. R. A. Palmans, A. Heise, *Enzymatic Polymerisation*, Springer, Berlin/New York **2010**.
[23] H. N. Cheng, R. A. Gross, *Green Polymer Chemistry: Biocatalysis and Biomaterials*, American Chemical Society, New York **2010**.
[24] S. Kobayashi, A. Makino, *Chem. Rev.* **2009**, *109*, 5288.
[25] J. van der Vlist, K. Loos, Transferases in Polymer Chemistry, in *Enzymatic Polymerisation* (Eds: A. R. A. Palmans, A. Heise), Springer, Berlin/New York **2011**.
[26] J. van der Vlist, K. Loos, Enzymatic Polymerizations of Polysaccharides, in *Biocatalysis in Polymer Chemistry* (Ed: K. Loos), Wiley, New York/Chichester, UK **2010**, Ch. 9.
[27] J. Kadokawa, *Chem. Rev.* **2011**, *111*, 4308.
[28] S. Shoda, R. Izumi, M. Fujita, *Bull. Chem. Soc. Jpn.* **2003**, *76*, 1.
[29] W. Kloosterman, S. Roest, S. Priatna, E. Stavila, K. Loos, *Green Chem.* **2013**, DOI: 10.1039/C3GC41115J
[30] K. Loos, V. von Braunmühl, R. Stadler, K. Landfester, H. W. Spiess, *Macromol Rapid Commun* **1997**, *18*, 927.
[31] H.-G. Breitinger, *Tetrahedron Lett.* **2002**, *43*, 6127.
[32] J. van der Vlist, I. Schönen, K. Loos, *Biomacromolecules* **2011**, *12*, 3728.
[33] L. Iwanoff, *Ber. deutsch. Bot. Ges.* **1902**, *20*, 366.
[34] J. Bodar, *Biochem. Z.* **1925**, *165*, 1.
[35] C. F. Cori, S. P. Colowick, G. T. Cori, *J. Biol. Chem.* **1937**, *121*, 465.
[36] W. N. Emmerling, B. Pfannemüller, *Makromol. Chem., Macromol. Chem. Phys.* **1978**, *179*, 1627.
[37] E. Husemann, M. Reinhardt, *Makromol. Chem.* **1962**, *57*, 109.
[38] E. Husemann, M. Reinhardt, *Makromol. Chem.* **1962**, *57*, 129.
[39] K. Loos, R. Stadler, *Macromolecules* **1997**, *30*, 7641.
[40] K. Loos, A. Böker, H. Zettl, A. F. Zhang, G. Krausch, A. H. E. Müller, *Macromolecules* **2005**, *38*, 873.
[41] K. Loos, A. H. E. Müller, *Biomacromolecules* **2002**, *3*, 368.
[42] J. Van der Vlist, M. Faber, L. Loen, T. J. Dijkman, L. A. T. W. Asri, K. Loos, *Polymers* **2012**, *4*, 674.
[43] R. F. Borch, M. D. Bernstein, H. D. Durst, *J. Am. Chem. Soc.* **1971**, *93*, 2897.
[44] M. Yalpani, D. E. Brooks, *J. Polym. Sci., Part A* **1985**, *23*, 1395.
[45] J. van der Vlist, M. P. Reixach, M. van der Maarel, L. Dijkhuizen, A. J. Schouten, K. Loos, *Macromol. Rapid Commun.* **2008**, *29*, 1293.
[46] T. H. Silva, V. Garcia-Morales, C. Moura, J. A. Manzanares, F. Silva, *Langmuir* **2005**, *21*, 7461.
[47] S. M. Mendoza, I. Arfaoui, S. Zanarini, F. Paolucci, P. Rudolf, *Langmuir* **2006**, *23*, 582.
[48] D. A. Shirley, *Phys. Rev. B* **1972**, *5*, 4709.
[49] A. Ulman, *Chem. Rev.* **1996**, *96*, 1533.
[50] M. M. Pollard, M. Lubomska, P. Rudolf, B. L. Feringa, *Angew. Chem. Int. Ed.* **2007**, *46*, 1278.
[51] D. G. Castner, K. Hinds, D. W. Grainger, *Langmuir* **1996**, *12*, 5083.
[52] M. T. Lee, C. C. Hsueh, M. S. Freund, G. S. Ferguson, *Langmuir* **1998**, *14*, 6419.
[53] M. Wirde, U. Gelius, L. Nyholm, *Langmuir* **1999**, *15*, 6370.
[54] *Practical Surface Analysis: Auger and X-Ray Photoelectron Spectroscopy;*, Wiley, Chichester, UK **1990**.
[55] A. E. Hooper, D. Werho, T. Hopson, O. Palmer, *Surf. Interface Anal.* **2001**, *31*, 809.
[56] T. Fukui, S. Shimomura, K. Nakano, *Mol. Cell. Biochem.* **1982**, *42*, 129.
[57] H. C. Ho, J. H. Wang, *Biochemistry* **1973**, *12*, 4750.
[58] J. Ciric, K. Loos, *Carbohydr. Polym.* **2013**, *93*, 31.
[59] J. Ciric, J. Oostland, J. W. de Vries, A. J. J. Woortman, K. Loos, *Anal. Chem.* **2012**, *84*, 10463.
[60] J. Ciric, A. J. J. Woortman, P. Gordiichuk, M. C. A. Stuart, K. Loos, *Starch* **2013**, DOI: 10.1002/star.201300063
[61] W. T. Winter, A. Sarko, *Biopolymers* **1974**, *13*, 1461.
[62] V. G. Murphy, *Biopolymers* **1975**, *14*, 1487.
[63] G. Rappenecker, P. Zugenmaier, *Carbohydr. Res.* **1981**, *89*, 11.
[64] J. Brisson, H. Chanzy, W. T. Winter, *Int. J. Biol. Macromol.* **1991**, *13*, 31.
[65] S. Immel, F. W. Lichtenthaler, *Starch/Stärke* **2000**, *52*, 1.
[66] M. Tusch, J. Krüger, G. Fels, *J. Chem. Theory Comput.* **2011**, *7*, 2919.
[67] S. J. Kerber, J. J. Bruckner, K. Wozniak, S. Seal, S. Hardcastle, T. L. Barr, *J. Vac. Sci. Technol. A-Vac. Surf. Films* **1996**, *14*, 1314.